Nuclear Science and Techniques **21** (2010) 241–245

Simulation of heat transfer of supercritical water in obstacle-bearing vertical tube

ZHANG Bo SHAN Jianqiang* JIANG Jing

Schoocl of Nuclear Science and Technology, Xi'an Jiaotong University, Xi'an 710049, China

Abstract The heat transfer coefficient is very low at bulk temperatures higher than the pseudo-critical point, because the supercritical pressure leads to a vapor-like fluid. In this paper, the heat transfer downstream an obstacle-bearing vertical tube is simulated by the CFD code of Fluent 6.1, using an adaptive grid in the supercritical condition. The reliable results are obtained by the RNG k-ε model using the enhanced wall treatment. The blockage ratio and local temperature of obstacle affect greatly the heat transfer enhancement, and the resultant influence region and decay trend are compared with the existing equations.

Key words Supercritical water reactor, Obstacle, Enhancement, Heat transfer

1 Introduction

The supercritical water reactor (SCWR), essentially a water reactor, but operating at above critical point pressure, has been listed in the six candidates of the 4th generation nuclear power plant[1–4]. The heat transfer of supercritical fluid has been studied for several decades, on topics of e.g. the forced convective heat transfer[5], numerical analysis[6], deterioration of heat transfer[7,8] and reviews[9–11], and so on.

In recent years, due to limits in experimental conditions, test loops of supercritical water were numerically analyzed by commercial CFD codes. The studies using the Fluent code and turbulence models on two-dimensional upward flows in circular tubes at supercritical pressure showed that the renormalization-group k-ε model with enhanced wall treatment[12] can be selected as prediction model[13]. In Ref.[14], the heat transfer of supercritical water in channels was investigated using the CFX5.6 code, and the Reynolds Stress model of Speziale, Sarkar and Gatski (SSG) was recommended. Yang *et al*[15] showed that the two-layer model of Hassid and Poreh can achieve better prediction on the heat transfer of supercritical water in the low/high temperature region, and found a strong non-unifom temperature distribution along the circumferential direction of cladding. These results show that the heat transfer capability is strong in the region near pseudo critical point, and is weak outside this region, especially when the bulk temperature is above the pseudo-critical temperature of the vapor-like fluid.

In some SCWR designs, temperature of core outlet was set close to the pseudo-critical point to avoid the low heat transfer capability[16]. And the outlet temperature of reactor, which is restricted by the heat transfer capability of coolant, is crucial to the thermal efficiency of reactor. A better surface roughness, and a staircase type grid to induce the spiral flow, can enhance the heat transfer and decrease the cladding temperature[17]. In a light water reactor, the spacer is design for fixing up the reactor, enhancing the critical heat flux and increasing the heat transfer capability. The heat-transfer-increasing grid spacer has been investigated at sub-critical pressure condition. Yao *et al*[18] proposed a correlation for the enhancement of the down-stream heat transfer using a spacer grid with split-vane pairs. Based on the grid blockage ratio, Holloway *et al*[19] developed correlations of the heat transfer in a rod bundle down-

Supported by Xi'an Jiaotong Unversity (XJTU) and Atomic Energy of Canada Limited (AECL)
* Corresponding author. *E-mail address:* jqshan@mail.xjtu.edu.cn
Received date: 2009-12-16

stream of a standard support grid. The sub-critical pressure reactor has been studied by spacer grid effect for the heat transfer augmentation. However, the blockage ratio effect has not been reported in the supercritical condition due to limits in experimental conditions. In this paper, heat transfer phenomena downstream an obstacle-bearing vertical tube under supercritical condition is simulated with the commercial CFD code of Fluent 6.1.

2 Calculation model

Fig.1 shows schematically the model of a vertical tube in diameter of d and length of L. It is inserted with a segmented annular obstacle of stainless steel in thickness a (3 mm, in this paper) and height h, which is set as 1 mm in Section 3.3 to consider the effect of temperature on heat transfer augmentation. In section 3.2, we discussed effect of h on the heat transfer. The blockage ratio of the obstacle *vs* the flow area is defined as $\varepsilon_s = [1 - 4(d/2 - h)^2]/d^2$.

To analyze the turbulence model and the obstacle effect on heat transfer, we adopted the heat transfer in smooth tube conducted by Yamagata *et al.*[5] as the analytic basis. Of the 2-m long tube in 7.5 mm of inner diameter, the 1.5-m length was heated, and unheated 0.5-m length was at the entrance, to make sure that the flow is fully-developed at the section of heated inlet. The obstacle is 1 m away from the inlet. The computations was performed using CFD code Fluent 6.1 described by Fluent Inc.[20].

The two-dimensional axisymmetric model was used for axisymmetric circular tube with an annular obstacle. The discrete equations were solved by a non-uniform structure in the r-z grid system. In the r-direction, the grid of minimum thickness was adjacent to the wall and the radial mesh number was 50 to make non-dimensional length (y^+) lower than 1 at the largest Reynolds number, and the mesh width was 1.1 times larger toward the channel center. The mesh independence was verified by mesh numbers ranged from 2×10^4 to 2.1×10^5.

The uniform heat flux was imposed on inner surface of the tube. The obstacle was cooled by convection via the interface between the fluid and solid. There was no heat source in the obstacle, but heat conduction inside the obstacle was considered in the analysis. The inlet velocity was calculated by physical properties at its uniform temperature. The thermal physical properties at a constant pressure was calculated referring the data in IAPWS-IF97[21]. If the residuals of all equations at all computation nodes (including the nodes of energy, momentum, mass and turbulence), are less than 10^{-6} after the nth iteration, the solutions is assumed to be converged.

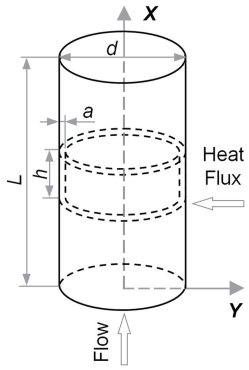

Fig.1 Geometry of the calculation model.

3 Results and discussion

3.1 Verification of numerical model

The RNG k-ε turbulent model was verified by comparing the simulation results with experimental data in smooth tube by Yamagata *et al*[5] (Fig.2). The heat transfer coefficients as a function of bulk temperature of 698 and 233 kW·m^{-2} were almost the same in the regions far from pseudo-critical point, and were enhanced in the region of pseudo-critical due to sharp changes in thermal properties in this region. Fig.2 shows that heat transfer coefficient can be predicted by the RNG k-ε turbulent model under the supercritical pressure[12,13].

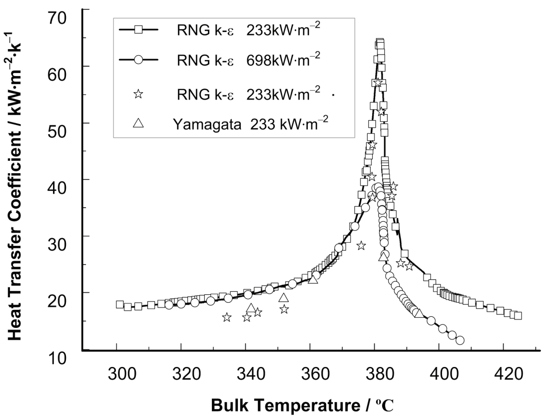

Fig.2 Measured and simulated heat transfer coefficient as a function of bulk temperature.

3.2 Effect of blockage ratio on heat transfer

Blockage ratios of 0.1, 0.2, 0.3, 0.4, 0.5 and 0.7 were modeled in the obstacle tube. Fig.3 shows the heat transfer coefficient as a function of bulk enthalpy at the 233-kW·m^{-2} heat flux. The bulk temperature at the obstacle position was at 356°C. As expected, a larger blockage ratio yielded a better enhancement of the heat transfer. The heat transfer coefficient at 0.7 blockage ratio was 2.5-times higher than the smooth tube, and it decayed in the downstream immediately to the value of the smooth tube. This is because of the broken boundary layers and the increased fluid velocity, which result in difficulty to reestablish the thermal boundary layers by fully mixing. On the other hand, a larger blockage ratio causes the pressure to drop. And both should be considered in design.

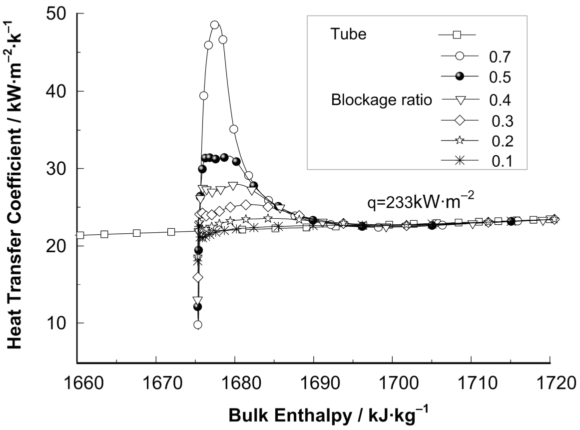

Fig.3 The heat transfer coefficient as a function of bulk enthalpy at the heat flux of 233 kW·m^{-2}.

In Refs.[18,19], the normalized length (x/d) is denoted as the decay distance, and the ratio of α to α_0 (α_0: benchmark of the heat transfer coefficient, x/d= 40) was used to indicate the enhancement effect. The heat transfer coefficient in a smooth tube was adopted as α_0. Fig.4 shows the enhancement of heat transfer decay at 698 kW·m^{-2} heat flux in the tube of different blockage ratios. When the local temperature was above the pseudo-critical temperature of 428°C and the enhancement ratio was about 3.2, the obstacle effect disappeared at $x/d \approx 30$. Figs.(3) and (4) show that the augmented peak is about 4 times of the tube diameter from the obstacle. This is consistent with the experimental data of Holloway *et al*[19].

3.3 Effect of local temperature on heat transfer augmentation

The enhancement ratio in Fig.4 is larger than in Fig.3. This is due to sharp thermo-physical changes. At 698 kW·m^{-2} heat fluxes, the bulk temperature was above the pseudo-critical point, the α_0 was small, and the velocity was large at low density, hence the easy occurrence of fluctuation and augmentation. Fig.5 shows the effect of local temperature on heat transfer with an obstacle of h=1 mm. The enhancement ratio increased with the bulk temperature, and the heat transfer coefficient was relative low above the pseudo-critical point due to vapor-like fluid, which is the limit of SCWR efficiency. The enhancement ratio near or above pseudo-critical point of the local temperature was larger than that below pseudo-critical point. Fig.6 verifies the heat transfer enhancement ratio varies with the bulk temperature at a constant heat flux and h=1 mm.

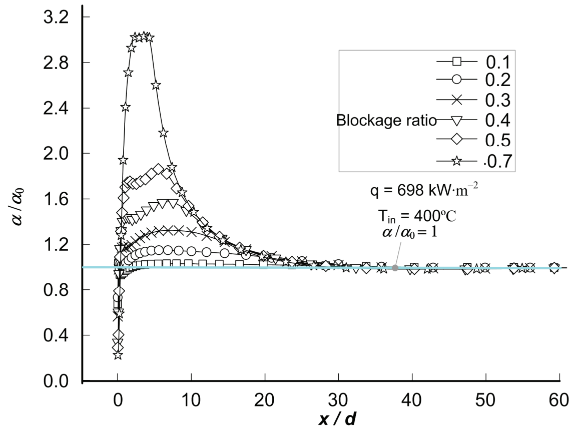

Fig.4 Enhancement of heat transfer decay downstream in the tube at 698 kW·m^{-2} heat flux.

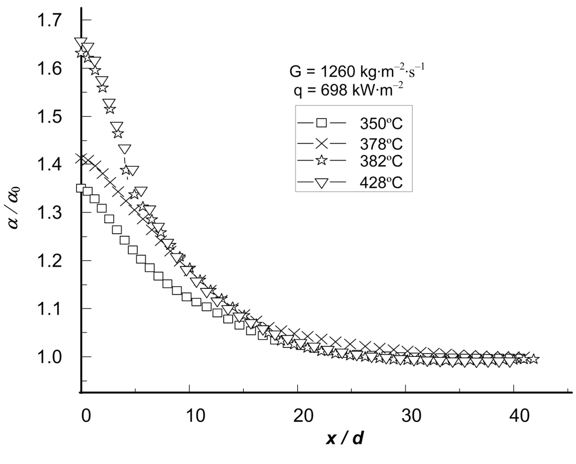

Fig.5 Augmented ratio at different bulk temperatures.

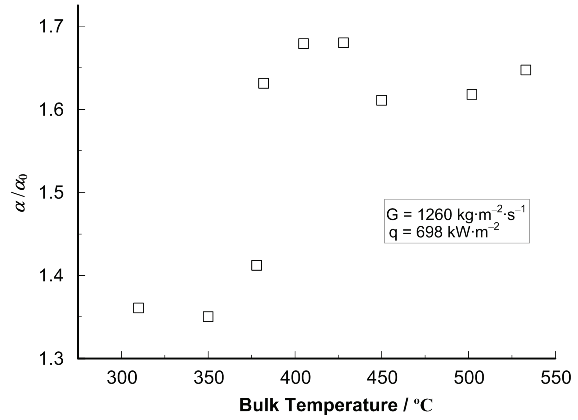

Fig.6 Enhancement ratio of heat transfer as a function of the bulk temperature at a constant heat flux.

3.4 Comparing the decay law with correlations

The decay law has been widely studied using the exponential and power laws[18,19], and Eq.(1)–(3) regarding the blockage ratio effect were compared with the simulation results.

$$Nu/Nu_0=1+5.55\varepsilon_s^{\,2}e^{-0.13(x/D_h)} \quad (1)$$

$$Nu/Nu_0=1+6.5\varepsilon_s^{\,2}e^{-0.8(x/D_h)} \quad (2)$$

$$Nu/Nu_0=1+3.0\varepsilon_s^{\,2}(x/D_h)^{-1.3} \quad (3)$$

where ε_s is blockage ratio of the obstacle *vs* the flow area, *Nu* is Nusselt number, *x* is the distance of the obstacle in the downstream (m), and D_h is hydraulic diameter (m). The above equations only consider the decay law in the region of $x/d > 4$. The decay law of the enhanced ratio is compared in Fig.7, and the results show that Eq. (1) gives reliable prediction.

4 Conclusions

Numerical simulation in an obstacle tube was carried out using CFD code Fluent 6.1 and adaptive grid using RNG *k*-*ε* model under the obstacle blockage ratio of 0.1–0.7. The RNG k-*ε* model with enhanced wall treatment can give a reliable prediction in the obstacle tube under supercritical condition. A larger blockage ratio enhances more in the heat transfer. The enhancement is related to local temperature due to the thermo-physical properties. The heat transfer augmentation ratio can be enlarged at the bulk temperature of above the pseudo-critical point to improve the thermo efficiency of supercritical water reactor. The equation of Yao *et al.*[18] is recommended to predict the decay law downstream of the obstacle.

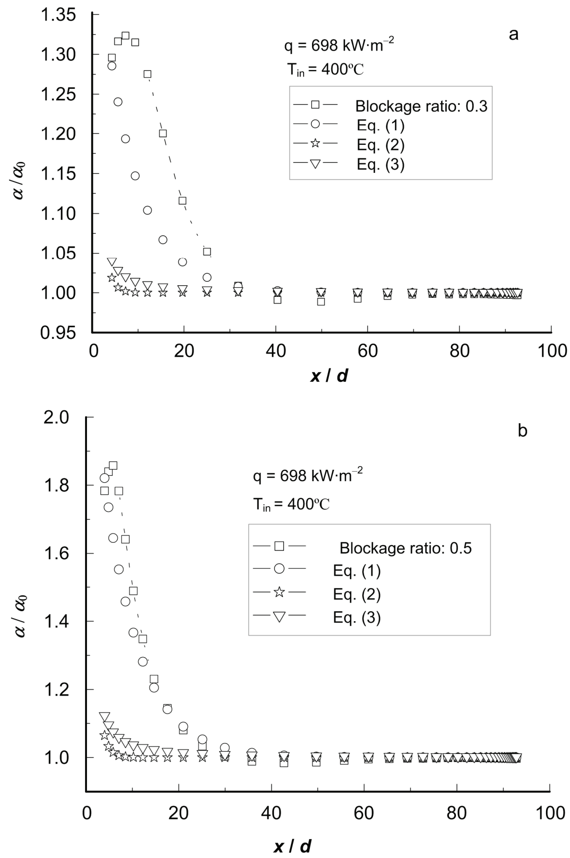

Fig.7 The decay law at different blockage ratios.

References

1 Oka Y, Koshizuka S. Proc of SCR-2000, Tokyo, Nov. 6–8, 2000, 101.

2 Yamaji A, Oka Y, Koshizuka S J. Nucl Sci Technol, 2005, **42:** 8–19.

3 Heusener G, Müller U, Schulenberg T, *et al.* Proc of SCR-2000, Tokyo, Nov. 6–8, 2000, 23–28.

4 Torgerson D F, Shalaby B A, Simon P. Nucl Eng Des, 2006, **236:** 1565–1572.

5 Yamagata K, Nishikawa K, Hasegawa S, *et al.* Int J Heat Mass Transfer, 1972, **15:** 2575–2593.

6 Kitou K, Koshizuka S, Oka Y. Nucl Technol, 2001, **135:** 252–264.

7 Shiralkar B, Griffith P. J Heat Trans, 1970, **92:** 465–474.

8 Koshizuka S, Takano N, Oka Y. Int J Heat Mass Trans, 1995, **38:** 3007–3084.

9 Cheng X, Schulenberg T. Scientific Report FZKA6609: heat transfer review, Forschungszentrum Karlsruhe, 2001.

10 Pioro I L, Khartabil H F, Duffey R B. Nucl Eng Des, 2004, **230:** 69–91.

11 Pioro I L, Duffey R B. Nucl Eng Des, 2005, **235:** 2407–2430.

12 Kim S H, Kim Y I, Bae Y Y, *et al.* Proc of ICAPP04, Pittsburgh, PA, USA, Jun.13–17, 2004, Paper 4047.

13 Roelof F, Komen, Ed. 21353/04.60811/P: CFD Analysis of heat transfer to supercritical water flowing vertically upward in a tube. Jahrestagung Kerntechnik, Nurnberg, Germany, May 10–12, 2005.

14 Cheng X, Kuang B, Yang Y H. Nucl Eng Des, 2007, **237:** 240–252.

15 Yang J, Oka Y, Ishiwatari Y, *et al.* Nucl Eng Des, 2007, **237:** 420–430.

16 Silin V A, Voznesensky V A, Afrov A M. Nucl Eng Des, 1993, **144:** 327–336.

17 Bastron A, Hofmeister J, Meyer L, Schulenberg T, *et al.* Proceedings of GLOBAL 2005, Tsukuba, Japan, Oct. 9 – 13, 2005.

18 Yao J, Hochreiter L E, Leech W J. ASME J Heat Transfer, 1982, **104:** 76–81.

19 Holloway M V, McClusky H L, Beasley D E. ASME J Heat Transfer, 2004, **126:** 43–53.

20 Fluent Inc. FLUENT 6.0 User's guide, Fluent Inc., USA, 2001.

21 Wagner W, Cooper J R, Dittmann A, *et al.* ASME J Eng Gas Turbines Power, 2000, **122:** 150–182.